CRYSTAL GROWTH & DESIGN
2009
VOL. 9, NO. 6
2927–2936

Structural Transitions and Flexibility during Dehydration−Rehydration Process in the MOF-type Aluminum Pyromellitate $Al_2(OH)_2[C_{10}O_8H_2]$ (MIL-118)

Christophe Volkringer,[†] Thierry Loiseau,*[,†] Nathalie Guillou,[†] Gérard Férey,[†,‡] Mohamed Haouas,[§] Francis Taulelle,[§] Nathalie Audebrand,[||] Irene Margiolaki,[⊥] Dmitry Popov,[⊥] Manfred Burghammer,[⊥] and Christian Riekel[⊥]

Institut Lavoisier (UMR CNRS 8180), Institut Universitaire de France, Porous Solids Group & Tectospin Group, Université de Versailles Saint Quentin en Yvelines, 45, avenue des Etats-Unis, 78035 Versailles, Sciences Chimiques de Rennes (UMR CNRS 6226), Université de Rennes 1, avenue du Général Leclerc, 35042 Rennes cedex and ESRF, 6, rue Jules Horowitz, B.P. 220, 38043 Grenoble cedex, France

Received March 9, 2009; Revised Manuscript Received April 9, 2009

ABSTRACT: A new metal−organic framework (MOF)-type aluminum pyromellitate (MIL-118) has been hydrothermally synthesized in water at 210 °C for 24 h. The crystal structure of the as-synthesized phase ($Al_2(OH)_2(H_2O)_2[C_{10}O_8H_2]$ or MIL-118A) has been solved from single-crystal analysis using synchrotron radiation with a specific microdiffraction setup at ESRF ID13 beamline. It consists of infinite chains of trans-connected aluminum-centered octahedra linked to each other through the pyromellitate ligand. The organic linker is not fully connected, and one carboxyl oxygen of two carboxylate functions is hydrogen bonded to the terminal water molecule attached to aluminum cations. Upon heating of the sample, the structure analysis (from powder X-ray diffraction data) showed that the terminal water is removed and the previously nonbonded carboxylate groups are now linked to aluminum reflecting a solid-state transition with the formation of Al-OCO bonding ($Al_2(OH)_2[C_{10}O_8H_2]$ or MIL-118B). This dried phase is able to reversibly adsorb and desorb ambient water. This hydration process induces a second phase transition with the encapsulation of water molecules within the channels delimited by the infinite chains and the aromatic ligands. In the third hydrated phase ($Al_2(OH)_2[C_{10}O_8H_2]\cdot 2.75H_2O$ or MIL-118C), whose structure was solved from powder X-ray diffraction data collected at ESRF ID31), the inorganic chains are shifted to each other with $a \approx b/6$ translation along the b axis, corresponding to a tilt angle of 90° between the benzene rings and the chains, instead of 61° in the dried phase MIL-118B. A 36.5° rotation of the benzene rings is also observed along the c axis. The occurrence of such a flexible network (6% variation for cell volume) was fully characterized by X-ray thermodiffraction, thermogravimetric analysis, and solid-state NMR (^{27}Al, ^{1}H).

Introduction

The search for porous hybrid organic−inorganic crystalline materials is attracting an extensive interest due to the occurrence of rich and various three-dimensional (3D) architectures with tunable chemical and physical properties.[1−3] These compounds named metal−organic framework (MOF) or coordination polymers may exhibit many applications in the fields of storage, separation,[4] catalysis,[5,6] magnetism,[7] drug delivery,[1] and batteries.[8] They exhibit structures based on the extended connection of organic linkers with metallic clusters (also chains, or layers) generating infinite 3D topologies. The use of aromatic carboxylate spacers which provide strong M−O−C bonding was observed to induce robust and rigid networks; some of them are characterized by extra-large pore highly crystalline frameworks with very high apparent surface area values.[1,9]

Besides the variety of the linkers coming from the organic chemistry, most of the studies have been devoted to the reactivity with the divalent metals (mainly transition metals such as Cu or Zn), but the utilization of light trivalent metals (first raw of transition metals or Al, Ga...) has received little attention. Among them, aluminum metal studies have been much less reported for the synthesis of MOF-type solids, although cheap materials with relatively low density can be produced at the industrial scale. Indeed, in Férey's group, a few aluminum-based compounds have been isolated. They correspond to the aluminum terephthalate (MIL-53[10]), the aluminum naphthalene dicarboxylate (MIL-69[11]), and two aluminum trimesates (MIL-96[12] and MIL-110[13]). More recently, Comotti et al.[14] reported the preparation of an aluminum-based MOF phase with the ligand 1,4-naphthalenedicarboxylate ($Al(OH[1,4\text{-ndc}]\cdot 2H_2O$) consisting of a 3D network closely related to that of MIL-53. Other MIL-69 derivates have been also described by Kaskel.[15] In this course, we are continuing our investigations with the use of the pyromellitate ligand (1,2,4,5,-benzenetetracarboxylate). We have previously described several MOF-type solids based on the association of such a linker with different trivalent metals such as vanadium,[16] iron,[17] gallium,[18] or indium.[19] Other groups also reported different iron[20] or indium[21−23] pyromellitates exhibiting various network topologies. This contribution deals with the hydrothermal synthesis of a hydrated compound $Al_2(OH)_2(H_2O)_2[C_{10}O_8H_2]$ labeled MIL-118A (Materials Institut Lavoisier), which was analyzed by diffraction technique using synchrotron radiation from a microcrystal (ID13 at ESRF).[13] Its dehydration process was characterized by powder X-ray diffraction and upon water removal, a solid-state structural transformation into a second dried phase $Al_2(OH)_2[C_{10}O_8H_2]$ (MIL-118B) was observed, which induces the formation of a 3D network based on one-dimensional (1D) channels. The structure of the latter is closely related to that of the vanadium(III) or indium(III) pyromellitates MIL-60[16,19] and iron(II) pyromellitate MIL-66;[24] it is able to adsorb and desorb ambient

* To whom correspondence should be addressed. E-mail: loiseau@chimie.uvsq.fr. Phone: (33) 1 39 254 373. Fax: (33) 1 39 254 358.
[†] Institut Lavoisier, Porous Solids Group.
[‡] Institut Universitaire de France.
[§] Institut Lavoisier, Tectospin.
[||] Sciences Chimiques de Rennes.
[⊥] ESRF.

10.1021/cg900276g CCC: $40.75
Published on Web 05/07/2009

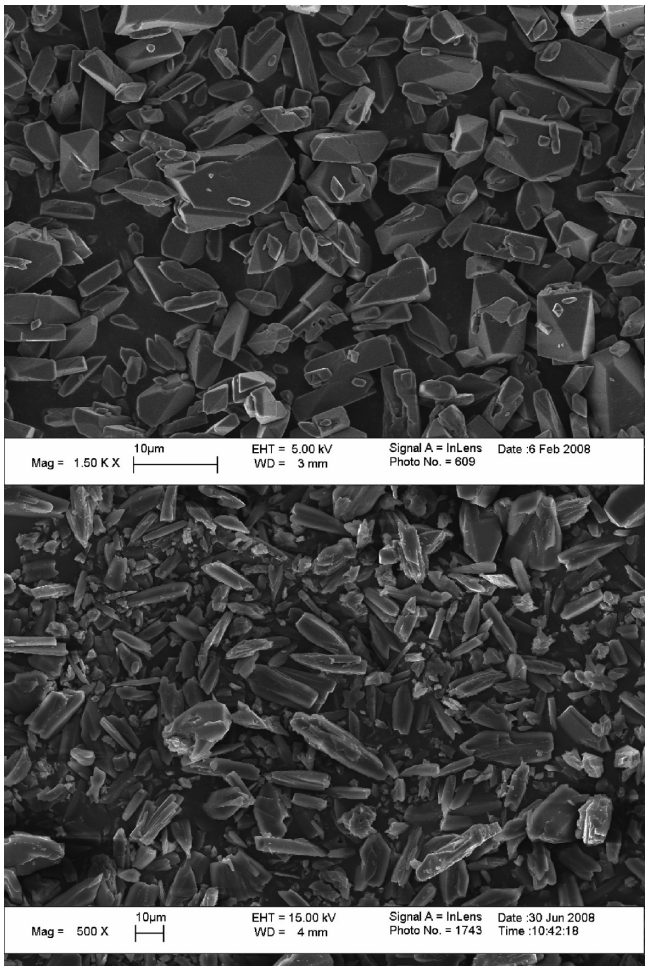

Figure 1. SEM photographs of the as-synthesized sample of MIL-118A (top) and the rehydrated sample of MIL-118C (bottom).

water molecules with some slight structural modifications (MIL-118C) reflecting a breathing effect of the network. The three forms of the aluminum pyromellitate MIL-118 were analyzed by solid-state NMR (^{27}Al, ^{1}H).

Experimental Section

Synthesis. The phase MIL-118A or $Al_2(OH)_2(H_2O)_2[C_{10}O_8H_2]$ was hydrothermally synthesized from a mixture of aluminum nitrate ($Al(NO_3)_3 \cdot 9H_2O$, Carlo Erba, 99+%), pyromellitic acid (1,2,4,5-benzenetetracarboxylic acid, noted H_4btec, $C_6H_2(CO_2H)_4$, Aldrich, 96%), and desionized water. The starting composition was 150 mg (0.4 mmol) of $Al(NO_3)_3 \cdot 9H_2O$, 50 mg (0.2 mmol) of H_4btec and 5 mL (277.8 mmol) of water, which was placed in a 23 mL Teflon-lined stainless steel Parr autoclave under autogenous pressure at 210 °C for 24 h. The starting and final pH values were 2.0 and 0.9, respectively. The resulting white powdered product (yield: 66% based on Al) was filtered off, washed with deionized water, and dried at room temperature. The SEM examination (LEO 1530 Gemini) showed that MIL-118A consists of tiny elongated prismatic crystallites of 2−15 μm size (Figure 1). Elementary chemical analysis: Al: 14.44%; C: 31.70%; H: 2.13%. Calculated chemical formula from $Al_2(OH)_2(H_2O)_2[C_{10}O_8H_2]$: Al: 14.43%; C: 32.08%; H: 2.20%.

The as-synthesized aluminum pyromellitate has been characterized by thermogravimetric and thermodiffraction analyses. Upon heating of the sample, a phase transition appeared from 170−180 °C and a second crystalline phase (called MIL-118B) was isolated in dry atmosphere. A sample of MIL-118A was calcined at 200 °C overnight, placed in a glass capillary (diameter 0.5 mm), and subsequently heated in an oven at 250 °C before sealing with glue, preventing water adsorption from the atmosphere. At room temperature, the MIL-118B phase is able to adsorb ambient water in air after a few days or in a desiccator over saturated water vapor after a few hours. The hydrated phase (MIL-118C) has been therefore identified. It was noticed that the direct reaction of MIL-118B in suspension with water systematically led to a mixture of the B and C forms, whatever the temperature treatment (ambient or hydrothermal conditions). The structures of the calcined (MIL-118B) and rehydrated forms (MIL-118C) were determined by means of powder X-ray diffraction. The sample of the rehydrated compound MIL-118C was examined by SEM (Figure 1), and this showed that elongated crystallites are still observed but with rougher surfaces and less defined faces, indicating the formation of surface microstrains during the dehydration−hydration process.

Single-Crystal X-ray Diffraction Analysis. A colorless needle-like crystal of MIL-118A (2−3 μm thickness) was selected and attached under an optical microscope by Araldite glue to a tapered glass capillary using a Kleindiek MM3A micromanipulator. Because of the small size of the crystals, no absorption correction was applied. Experiments were performed at the ESRF ID13 undulator beamline.[13] The beam was monochromated to $\lambda = 0.96130(6)$ Å by a liquid N_2 cooled Si-111 double crystal and focused to about 1 μm × 1 μm size by a crossed mirror system. In such a setup, the flux density at the sample within an about 1 × 1 μm^2 effective beam reaches up to 3.10^{10} photons/s/μm^2. The microgoniometer consisted of an air bearing spindle and a Kleindiek MM3A micromanipulator carrying a Hampton Research magnetic base. An Olympus microscope looking upstream along the beam path on the focus position was used for sample alignment in the focal spot. The optical alignment precision was below 1 μm. The crystal was rotated during data collection with an angular step of 1°. Diffraction patterns were recorded by a MAR 165 CCD detector with 2 K × 2 K pixels of 78.94 × 78.94 μm and 16 bit readout. The diffraction patterns were processed with XDS[25] software. Two data sets of 1 and 0.5 s per frame exposure time were collected on two different points of the sample and merged into one resulting data set of 0.9 Å highest resolution and $I/\sigma = 7.6$ using XSCALE program within the XDS package.

The structural model was found by direct method with SHELXS-86[26] software and developed by successive difference Fourier syntheses using SHELXL-97.[27] Hydrogen atoms belonging to the benzene ring were refined using geometric constraints. Crystallographic data and parameters are presented in Table 1.

Powder X-ray Diffraction Analysis. The structure determinations of the calcined (MIL-118B) and rehydrated (MIL-118C) forms were carried out from X-ray powder diffraction data. Each sample was introduced into a 0.5 mm capillary. The pattern of MIL-118B was scanned at room temperature on a Bruker D8 Advance diffractometer with a Debye−Scherrer geometry, in the range $2\theta = 8-80°$ with a step length of 0.015° (2θ) and a counting time of 322 s·step^{-1}. The D8 system is equipped with a Ge(111) monochromator producing Cu Kα_1 radiation ($\lambda = 1.540598$ Å) and a SOL-X detector. X-ray powder diffraction data of MIL-118C were collected on ID31 of the ESRF. The beamline receives X-rays from the synchrotron source (which operates with an average energy of 6 GeV and a current beam of typically 100 mA) from an undulator device. The incident X-ray wavelength was 0.79990(6) Å using an incident beam size of 2.0 mm (horizontal) × 1.0 mm (vertical). The sample was rapidly spun during data collection to ensure good powder averaging. Extractions of the peak positions, pattern indexing, Fourier calculations, and Rietveld refinements were carried out with the TOPAS[28] program. Unit cells and space groups were found unambiguously by the LSI-indexing method with satisfactory figures of merit ($M_{20} = 29$ for MIL-118B and $M_{20} = 102$ for MIL-118C).

Calculations were performed with the EXPO[29] package on both phases, using EXTRA for extracting integrated intensities and SIR*97* for direct methods structure solution. Lists of 159 and 199 reflections were extracted in the angular ranges 8−70° (2θ) and 2−38° (2θ) for MIL-118B and MIL-118C, respectively. According to the degree of diffraction overlap, about 49% of these reflections were statistically considered as independent. The whole structural frameworks were found unambiguously from the E-map with the highest figure of merit in both cases. Moreover, the nondisordered water molecule (Ow1) was also found from direct methods and Ow2 was localized from difference Fourier maps for MIL-118C. The anisotropic line broadening effect was modeled by using spherical harmonics series. Soft restraints were maintained on distances within the organic ligand (MIL-118B and MIL-118C) and Al−O bonds (MIL-118C). The final Rietveld plots

Table 1. Crystal Data and Structure Refinements for the Aluminium Pyromellitate MIL-118A (As-Synthesized), MIL-118B (Dehydrated Calcined Form) and MIL-118C (Rehydrated Form)

	MIL-118A	MIL-118B	MIL-118C
chemical formula	$Al_2(OH)_2$ $(H_2O)_2[C_{10}O_8H_2]$	$Al_2(OH)_2[C_{10}O_8H_2]$	$Al_2(OH)_2[C_{10}O_8H_2]\cdot 3H_2O$
formula weight	376.15	338.08	774.13
device	ID13 at ESRF	Bruker-D8	ID31 at ESRF
temperature	100 K	RT	RT
wavelength (Å)	0.96130(6)	1.540598	0.79990(6)
symmetry	monoclinic	orthorhombic	orthorhombic
space group	*C2/c*	*Pbam*	*Pnam*
a (Å)	11.365(3)	11.3322(13)	12.1320(1)
b (Å)	6.822(2)	6.6189(1)	6.61928(5)
c (Å)	17.733(2)	8.7217(2)	17.2271(2)
β (°)	90.62(4)		
V (Å^3)	1374.8(6)	654.18(3)	1383.42(2)
Z, calculated density	4, 1.817	2, 1.696	4, 1.834
adsorption coefficient	0.281 mm^{-1}		
2θ range (°)	9.42 to 62.3	8.0 to 79.5	4.0 to 46.0
reflections collected	6004		
unique reflections	652	218	727
goodness of fit	1.771	1.29	1.63
no. structural parameters	109	20	46
no. atoms	13	7	15
R_{sym}[a]	0.261		
$R_{mrgd\text{-}F}$[a]	0.126		
R indices [$I > 2\sigma(I)$]	$R_1 = 0.1127$, $wR_2 = 0.2710$		
R indices (all data)	$R_1 = 0.1227$, $wR_2 = 0.2780$		
R free [$I > 2\sigma(I)$]	$R_1 = 0.1122$		
R free (all data)	$R_1 = 0.1294$		
no. profile parameters		31	32
Rwp		0.061	0.070
R_P		0.046	0.052
R_{Bragg}		0.011	0.030

[a] After Diederichs, K; Karplus, P. *Nat. Struct. Biol.* **1997**, *4*, 269.

(Figure 2) correspond to satisfactory model indicators and profile factors (see Table 1). A small amount of MIL-118B (about 4 wt %) was detected and taken into account in the Rietveld refinement of the MIL-118C.

In situ thermodiffraction experiments were carried out on a Bruker AXS D5005 powder diffractometer using a diffracted-beam-graphite monochromator (Cu K$\alpha_{1,2}$) and equipped with an Anton Paar HTK1200 oven camera. X-ray powder diffraction data were collected in air between 20 and 600 °C over the angular range 2−38° (2θ) with a counting time of 4 s·step^{-1} and a step length of 0.04° (2θ).

Thermogravimetric Analysis. The TG experiments were carried out on a TA Instruments type 2050 thermoanalyzer TA under oxygen gas flow with a heating rate of 1 °C·min^{-1}.

Solid-State NMR. ^{27}Al and ^{1}H MAS NMR spectra were recorded with the Bruker Avance 500WB spectrometer operating at 11.7 T. The spinning frequency used was 30 kHz. ^{27}Al spectra were recorded at Larmor frequency of 130.315 MHz relative to an aqueous solution of $Al(NO_3)_3$ with 0.4 μs pulses and 0.1 s recycling time. ^{1}H spectra were recorded at Larmor frequency of 500.133 MHz relative to TMS with 4.6 μs pulses and 4 s recycling time. ^{1}H 2D DQ MAS experiments were performed with four cycles of the back-to-back (BABA) recoupling sequence.[30] The t_1 increments were set equal to one rotor period. In the transfer population in double resonance (TRAPDOR) NMR experiments,[31,32] a spin echo pulse was applied to the I (^{1}H) channel with simultaneous irradiation of aluminum (close to on-resonance conditions) during the first period of evolution time (τ). In theory, the continuous irradiation reintroduces the effects of the heteronuclear dipolar coupling that are normally removed by magic-angle sample rotation. Two experiments, that is, without and with ^{27}Al irradiation, are performed for one rotor cycle, and the difference between these two spectra reveals the signals of the protons in close proximity to aluminum atoms. An ^{27}Al radio frequency (rf) field amplitude of 126 kHz was used. ^{27}Al MQMAS NMR experiments were performed with the standard Z-filter scheme, a single CW pulse for excitation of triple quantum (3Q) coherences and FAM II sequence[33] for 3Q → 0Q conversion. The excitation and refocusing pulses were obtained using a rf field of 114 kHz, whereas the selective $\pi/2$ pulse in the *Z*-filter used a rf field of 4.5 kHz. The dwell time in t_1 (isotropic) dimension of MQMAS measurements was synchronized with the spinning rate of the rotor. Data acquisitions were performed using 4128 scans per t_1 step and a 0.1 s delay between scans. All measurements were taken at room temperature on three samples from a same parent batch of MIL-118A. The MIL-118A sample was divided in two parts, one part for NMR measurements as it, the other to prepare MIL-118B and MIL-118C NMR samples. A pretreatment of this later at 250 °C for 12 h was first carried out. The 2.5 mm zirconium oxide NMR rotor was then filled, with a part of the resulting phase MIL-118B, as fast as possible avoiding long contact time with ambient air. Before sealing the rotor with the caps (top and bottom), further treatment of the sample inside the opened rotor at 250 °C for 4 h was conducted. NMR measurements were then realized immediately. The other part of MIL-118B was placed in a closed desiccator containing a saturated solution of NaCl during 72 h in order to get the NMR sample of MIL-118C.

Results

Crystal Structure of the As-Synthesized Aluminum Pyromellitate $Al_2(OH)_2(H_2O)_2[C_{10}O_8H_2]$ (MIL-118A). The structure of $Al_2(OH)_2(H_2O)_2[C_{10}O_8H_2]$ (or MIL-118A) is built up from the connection of btec ligands with infinite chains of trans-connected aluminum-centered octahedra (Figure 3). It consists of one unique crystallographical site for aluminum, which is coordinated to three carboxyl oxygen atoms (Al1−O1 = 1.890(6), Al1−O3 = 1.925(6) and Al1−O4 = 1.908(6) Å), two hydroxyl groups in trans position (Al1−O2 = 1.851(5) Å), and a terminal water molecule (Al1−O5 = 1.943(7) Å). The assignments of the hydroxyl groups and water molecules to the oxygen atoms O2 and O5, respectively, are in good agreement with the valence bond[34] calculations (calculated value for O2: 1.163, expected: 1.2; for O5: 0.454, expected: 0.4), although no hydrogen atom was revealed from the Fourier maps analyses by X-ray diffraction. The aluminum-centered octahedra are connected to each other by sharing μ_2-OH corners in order to generate infinite straight chains running along the *b* axis (Figure 3). Such an inorganic motif is commonly observed in other MOF-type compounds incorporating aluminum (MIL-53,[10]

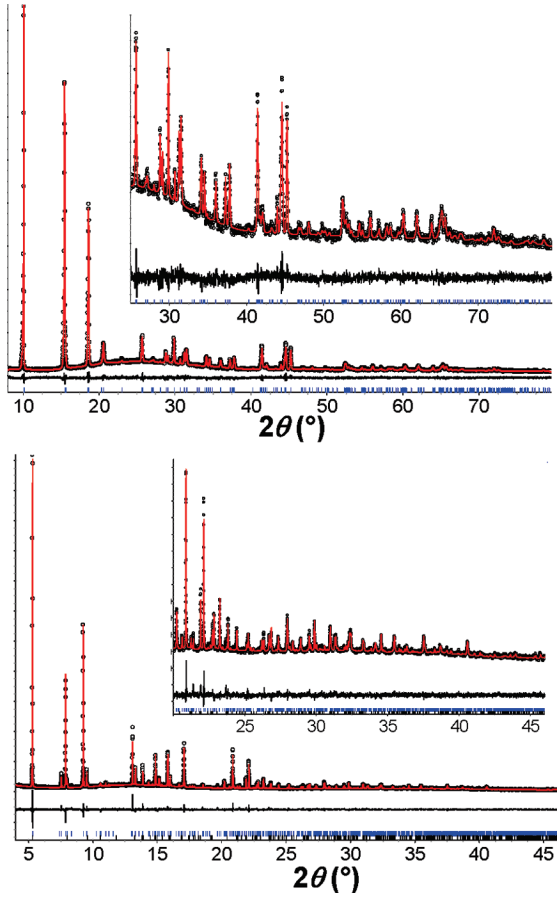

Figure 2. The final Rietveld plots as a function of $2\theta°$ of the MIL-118B (top) and MIL-118C (bottom) compounds. Observed data are shown by circles; the calculated pattern is displayed by the red solid line; the lower black curve is a plot of the difference, observed minus calculated.

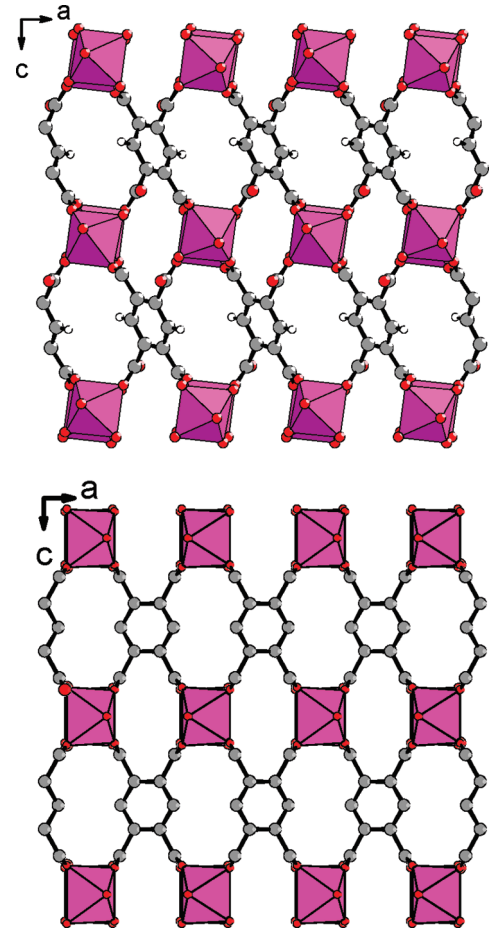

Figure 3. (top) View of the structure of $Al_2(OH)_2(H_2O)_2[C_{10}O_8H_2]$ (MIL-118A) along the *b* axis showing the pyromellitate ligand linking the aluminum-centered octahedra. (bottom) Structure of its dehydrated calcined form $Al_2(OH)_2[C_{10}O_8H_2]$ (MIL-118B) showing the pyromellitate linker fully connected to four distinct chains of the octahedrally coordinated aluminum atoms.

MIL-69[11]) or other trivalent metals.[1] The 3D cohesion of the structure is ensured by the connection of the four inorganic chains through the carboxylate groups of the btec linkers in the (a, c) plane (Figure 3). However, in MIL-118A, the pyromellitate ligand adopts a specific connection type since two carboxylates groups are coordinated to two adjacent aluminum atoms in a bidentate bridging mode (C1−O1 = 1.262(10) and C1−O4 = 1.253(10) Å) and the two other carboxylate groups are coordinated only to one aluminum atoms in a monodentate fashion (C3−O3 = 1.281(10) Å). The last C−O bond occurs in its deprotonated form with a distance of 1.249(12) Å (C3−O6). In the case of the presence of proton attached to terminal C−O bond, typical larger distances of 1.31−1.32 Å are observed as in the aluminum fluoride $Al_2F_8 \cdot (pyr)_2 \cdot H_3btc$,[35] crystallizing with the trimesic acid species. Moreover, the infrared spectrum of MIL-118A does not show any vibration bands in the 1720−1700 cm^{-1} region corresponding to CO_2H (see Supporting Information). Only the $\nu_{as}(\text{-}CO_2)$ and $\nu_s(\text{-}CO_2)$ adsorption peaks are visible in the range 1637−1387 cm^{-1}. The organic linker is connected to six aluminum centers with the bidentate and monodentate modes in strict alternation within the benzene ring (Figure 4). This particular configuration (μ_6-η^1:η^1:η^1:η^1:η^1:η^1) was not reported in the other trivalent metal pyromellitates. Only the bidentate bridging mode was observed in MIL-61,[16,18,21] MIL-60,[19] MIL-82,[17,20] or the $In_3(OH)_2[C_{10}O_8H_2]_2$[22] series. The remaining nonbonded carboxyl oxygen preferentially interacts though strong hydrogen bond (C3−O6···O5−Al = 2.66(2) Å) with the terminal water molecule attached to aluminum. It results in a slightly larger Al−OH−Al angle in the inorganic chains (135.1(3)°) compared to the other aluminum carboxylates MIL-53[10] (from 124.9(1) to 132.3(1)°), MIL-69[11] (130.81(1)°) or $Al(OH)(1,4\text{-ndc}) \cdot 2H_2O$[14] (120.8(3)°), in which only the bidentate bridging mode exists.

The thermal behavior of the as-synthesized aluminum pyromellitate was analyzed by both thermogravimetric and thermodiffraction techniques. The TG curve (Figure 5) shows two events between 100 and 600 °C. The first weight loss up to 250 °C is assigned to the departure of terminal water species (observed: 11.2%; expected: 9.6%). The slight difference of weight loss values might be due to extra water adsorbed on the powered sample. The second weight loss from 400−420 to 550 °C corresponds to the removal of the organic linker together with the decomposition of the structure (observed: 63.1%; expected: 61.8%). The final residue is Al_2O_3 (observed: 27.0%; expected: 27.3%). These different steps have been followed by thermodiffraction (see Supporting Information). It appears that the departure of the bonded water molecules induces a phase transition with the formation of a very well crystallized phase corresponding to the dehydrated calcined form of the aluminum pyromellitate $Al_2(OH)_2[C_{10}O_8H_2]$ (or MIL-118B) between 150 and 170 °C. Bragg peaks of the latter are visible up to 495 °C, and its structure was further characterized by powder X-ray diffraction. Upon removal of the btec ligand, X-ray diffraction (XRD) powder pattern shows that the resulting phase is poorly

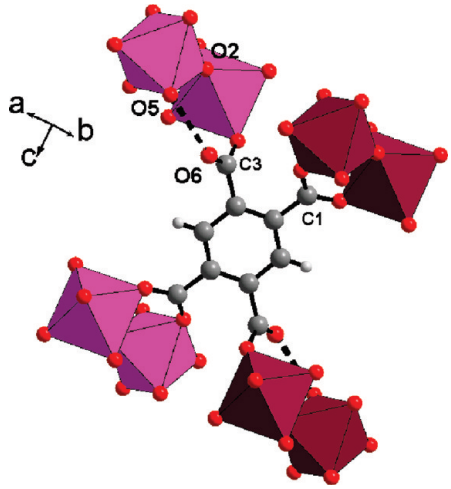

Figure 4. Connection mode of the pyromellitate ligand (μ_6-η^1:η^1:η^1:η^1:η^1:η^1) in MIL-118A, showing the strict alternation of the bidentate and monodentate bridges of the carboxylate function with the aluminum atoms belonging to four distinct chains of octahedra. Al octahedra have different colors for clarity. Dashed line indicates the hydrogen bond between carboxyl oxygen and terminal water attached to aluminum cations.

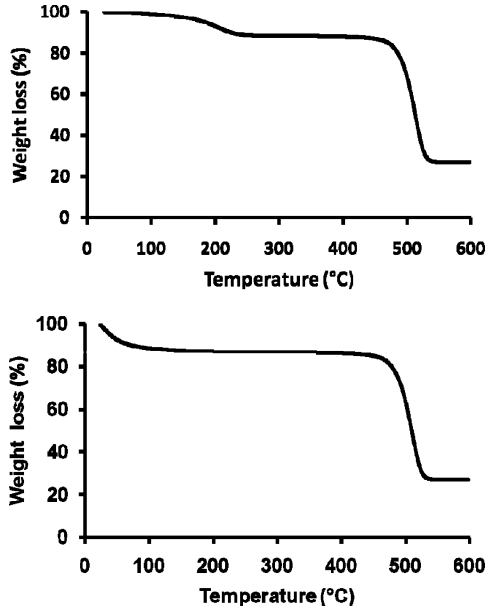

Figure 5. TG curves of MIL-118A (top) and MIL-118C (down), under O_2 gas flow, 1 °C·min^{-1}.

crystallized with some Bragg peaks assigned to the aluminum oxide δ-Al_2O_3 form (PDF file 47-1770).

Crystal Structure of the Dehydrated Calcined Aluminum Pyromellitate $Al_2(OH)_2[C_{10}O_8H_2]$ (MIL-118B). The structure of the second form of the aluminum pyromellitate is closely related to the previous hydrated one. It is composed of identical trans-connected infinite chains of aluminum-centered octahedra linked to the btec ligand. However, the departure of the terminal water species attached to aluminum atoms induces the rotation of the benzene ring in order to create a bond between the aluminum and the remaining free carboxyl oxygen (Figure 6), whereas a hydrogen bond type occurred between this C−O bond and the water in MIL-118A. This solid-state structural transformation results in the formation of a 3D structure with only a bidentate connection mode of the four carboxylate groups of

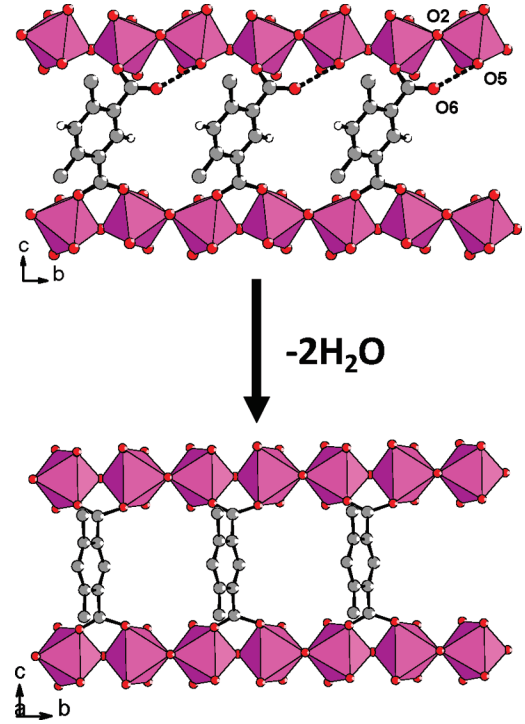

Figure 6. (top) Representation of the connection of the pyromellitate linker between two infinite trans-connected chains of aluminum octahedra running along the [010] direction in MIL-118A and MIL-118B (down). In MIL-118A, hydrogen bond interactions (dashed line; O5···O6 = 2.65(2) Å) occur between the terminal water molecule attached to aluminum cation (O5) and the remaining free carboxyl oxygen (O6), whereas a C−O−Al bonding is observed in MIL-118B due to the removal of the terminal water species. For each view, only two carboxylate groups of the tetradentate linker are shown for clarity.

the btec linker, which adopts the configuration μ_8-η^1:η^1:η^1:η^1:η^1:η^1:η^1:η^1. Therefore, the aluminum is octahedrally coordinated to four carboxyl oxygen atoms (Al−O = 1.850(7)−1.914(7) Å) and two bridging hydroxyl μ_2-OH groups (Al−O = 1.84(1)−1.88(1) Å) in trans position. The Al−OH−Al angle is 125.9(6)° and close to that found in previous aluminum-based MIL-n compounds (MIL-53, MIL-69) built up from infinite inorganic chains. Each organic ligand is connected to four distinct inorganic chains, delimiting small empty channels (3.5 × 1.5 Å^2) running along the *c* axis. The 3D framework is closely related to that encountered in the vanadium or indium MIL-60[16,19] and iron pyromellitates MIL-66[24] with the same metal/btec ratio of 2/1. The only difference is the angle of the aromatic ring with the inorganic chain, which is close to 90° in MIL-60 (V, In) or MIL-66 (Fe) and 61° in MIL-118B (Figure 7). From this observation, the network of MIL-118B is considered as a shrunk configuration of the MIL-60 one, with a shift of ≈*b*/6 of one chain to an adjacent one in the (*a*,*b*) plane. One may notice that upon heating, such a solid state formation of M-OCO bonding is quite rare in the MOF family. Nevertheless, the thermal process involving the topochemical transformation of hydrogen-bond interaction into covalent metal−carboxyl oxygen bonding was previously described by Vitall[36] in a series of zinc[37] and copper[38] carboxylates with the *N*-(2-hydroxybenzyl)-L-alanine ligand. Upon heating up to 120 °C, the terminal aquo species bonded to the divalent metal is removed, and it resulted in the formation of M−OCO bond together with the generation of a 3D open-framework coordination polymer.

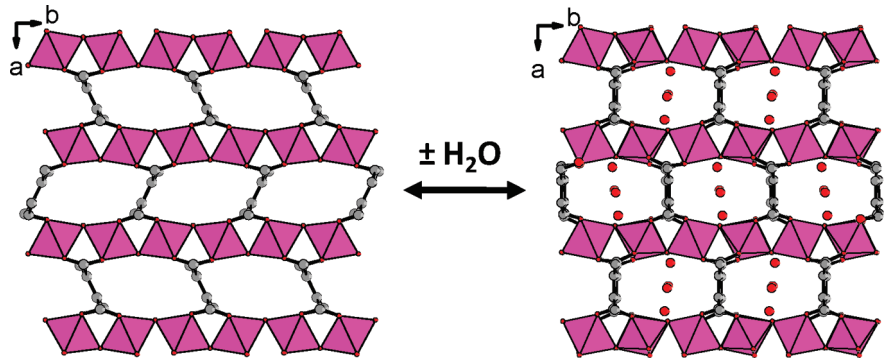

Figure 7. Representation of the network flexibility of MIL-118 upon water adsorption: View of the structure of the calcined form MIL-118B ($Al_2(OH)_2[C_{10}O_8H_2]$) (left) and its hydrated form MIL-118C ($Al_2(OH)_2[C_{10}O_8H_2]\cdot 2.75H_2O$) along the *c* axis, showing the 1D channels delimited by the infinite chains of metal-centered octahedra and the pyromellitate linkers. The water adsorption induces the shift of the inorganic chains to each other in order to get rectangular-shaped tunnels in the hydrated form, instead of lozenge-shape in the dried form. The network of the hydrated phase is similar to that of the vanadium or indium pyromellitate MIL-60.

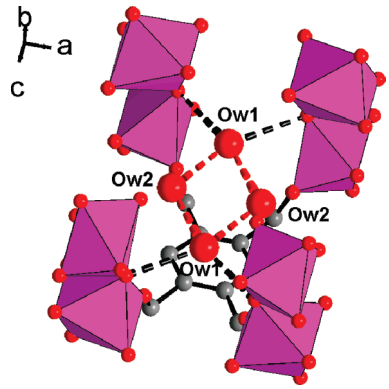

Figure 8. View of the hydrogen bond scheme of the water molecules and the inorganic chains in MIL-118C. Ow1 mainly interacts with μ_2-bridging OH groups and other molecules Ow2.

Crystal Structure of the Rehydrated Aluminum Pyromellitate $Al_2(OH)_2[C_{10}O_8H_2]\cdot 2.75H_2O$ (MIL-118C). Under air atmosphere, a new X-ray diffraction pattern is identified and differs from that of the as-synthesized compound MIL-118A. The structure of the third form of aluminum pyromellitate still reveals the connection of infinite chains of aluminum-centered octahedra with the btec ligand (Figure 7). The latter has a similar configuration μ_8-η^1:η^1:η^1:η^1:η^1:η^1:η^1:η^1 as found in the B form. Typical Al−O (from carboxyl oxygen) distances and Al−OH (μ_2-type bridging groups) are 1.84(1)−1.93(1) and 1.82(5)−1.95(2) Å, respectively. Although only one unique crystallographic Al sites was observed for the A and B forms, the hydrated phase C has two inequivalent crystallographic Al sites, residing on the special positions 4c. This structural feature was very well reflected by the solid-state ^{27}Al NMR analysis (see hereafter). The Fourier map analysis indicated the positions of two crystallographic sites (Ow1 and Ow2) assigned to water molecules coming from the hydration process and located within the channels of the structure, along the *c* axis (Figure 8). The Ow1 molecules mainly interact via hydrogen bonds with the bridging μ_2-hydroxyl groups between the aluminum cations (Ow1···O2 = 2.84(1) Å and Ow1···O1 = 2.96(1) Å) and with the second water species Ow2 (Ow1···Ow2 = 2.67(1) and 3.04(1) Å), which has a 50% site occupancy. Other hydrogen bonds interactions are also observed between Ow1 and the carboxyl oxygen atoms (Ow1···O3 = 2.91(2) Å; Ow1···O4 = 2.89(1) Å; Ow1···O5 = 2.97(1) Å). The second important structural feature is the observation of the variation of the tilt angle between the benzene ring of the btec linker and the inorganic chains. It was about 61° in the dried phase B but close to 90° in the hydrated form C, inducing $a \approx b/6$ shift of the chains along the *b* axis to each other (Figure 7). Moreover, the angle of two adjacent benzene planes along the *c* axis is

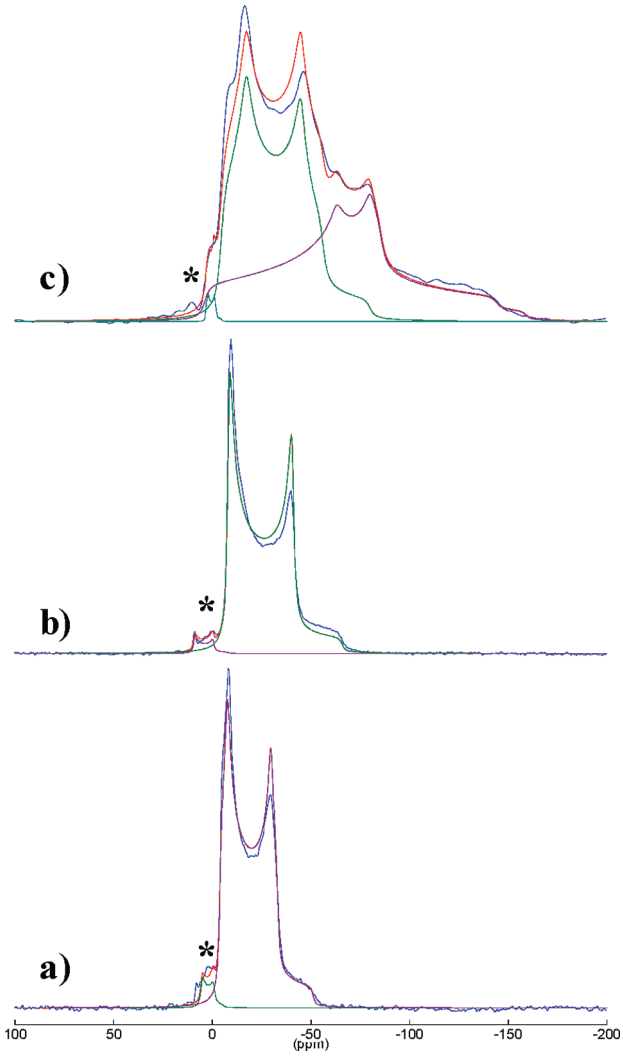

Figure 9. ^{27}Al MAS spectra of (a) MIL-118A, (b) MIL-118B, and (c) MIL-118C. All spectra were recorded at 130 MHz and spinning rate 30 kHz. Asterisks label the satellite transition and/or impurity signal.

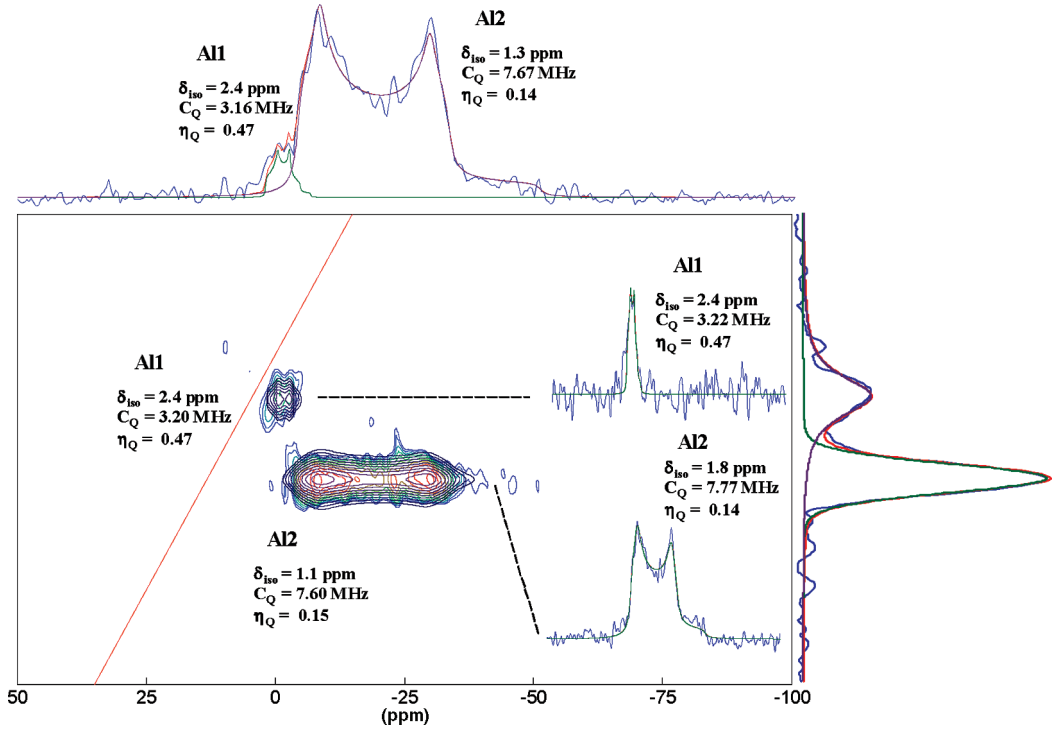

Figure 10. Contour plot of ^{27}Al 3QMAS NMR spectrum of MIL-118A collected at 11.7 T showing two signals, Al1 and Al2 as impurity and framework aluminum site, respectively. Similations of 2D slices, F1 and F2 projections as well as selected rows are presented.

around 73° in MIL-118B, whereas it is close to 0 in MIL-118C. This reflects that the aromatic cycles are rotated of 36.5° to each other along the *c* axis (73/2) during the water adsorption. Indeed, the hydrated form is identical to the other metal pyromellitates MIL-66 (Fe)[24] and MIL-60 (V, In).[16,19] In the latter compounds, water molecules are also found residing within the channels. Therefore, the water adsorption in MIL-118B is correlated to a second type of the structural changes with the shift of the inorganic chains to each other in order to accommodate the guest water species within the tunnels. A cell volume variation of ≈6% is observed with the water sorption.

The thermal behavior of the rehydrated form of the aluminum pyromellitate (MIL-118C) is characterized by two weight losses (Figure 5). As expected, the first event (30−120 °C) is assigned to the dehydration process, which corresponds to the departure of 2.75 H_2O per Al_2 unit (13.1%). This value is close to the water content estimated from the X-ray diffraction analysis, which converge to three H_2O per Al_2 unit. The MIL-118C framework is stable up to ≈400 °C and then collapses upon the removal of the organic linker (observed: 59.9%; expected: 62.5%). The final residue corresponds to δ-Al_2O_3 with the weight loss of 27.0%. The MIL-118C reversibly adsorbs and desorbs water when left in ambient air or heaed above 120 °C. The water desorption was characterized by X-ray diffraction as a function of temperature (see Supporting Information). From 65 °C, the water evacuation led to a change of the Bragg peaks with a well crystallized pattern corresponding to the dried phase MIL-118B. The dehydrated solid is stable up to 455 °C, and it was observed that the rehydration−dehydration process is reversible together with the structural modification reflecting a breathing effect for the MIL-118 network. This solid is able to adsorb water within the pores, generating hydrogen bonds interactions with the framework. These are strong enough to translate the inorganic chains in order to accommodate the tunnels space for its insertion.

This aluminum pyromellitate is a new example of network flexibility encountered in some MOF materials.[39−41] However, for MIL-118, the structural breathing amplitude (related to the cell volume change) is not so high in comparison with the values observed in the MIL-53 (50%) or MIL-88[1] (up to 230%) series. This might partly be due to the tetradentate linker in MIL-118 instead of the bidentate ligands in MIL-53 or MIL-88 compounds. The tetracarboxylate species would confer more rigidity in the framework with less internal degree of freedom for correlated rotations of the carboxylate arms. Nevertheless, the previous study reported in the MIL-53 network showed that the breathing amplitude coming from the water removal is not only due to the temperature but also to the nature of the metallic cation and drastic differences of the breathing behavior have been observed for the series Cr, Fe, Al, Ga for instance.[42−44] For MIL-118, identical effect is observed since only the aluminum-based structure exhibits such a flexibility. Its hydrated parent structures, MIL-60,[16,19,45] did not show any structure modification upon dehydration, reflecting no network breathing. Again, with this new example of flexible MIL-118/MIL-60 network, the nature of the cation does play a significant role in the fine-tuning of the open-framework expansion depending on the encapsulated molecules.

Solid-State NMR. Structural analyses of the MIL-118 compounds have been further studied by means of solid-state NMR techniques. ^{27}Al MAS NMR spectra, provided in Figure 9, showed a single signal for MIL-118A and MIL-118B, whereas two signals can be distinguished for MIL-118C. These results are fully consistent with the crystallographic data for which an unique Al site was found either in MIL-118A or MIL-118B. The two nonequivalent Al sites in MIL-118C were used to complete the choice of a consistent space group between the diffraction and NMR techniques. An additional small signal at around 2 ppm is present for the MIL-118A sample as revealed by the MQMAS spectrum (see Supporting Information), which

Table 2. Relative Intensities and Line-Shape Parameters Corresponding to ^{27}Al MAS Spectra of MIL-118 Samples

sample	δ_{iso} (ppm)[a]	C_Q (MHz)[a]	η_Q[a]	relative area (%)[a]
MIL-118A	1.8	7.7	0.13	100
MIL-118B	1.2	8.7	0.00	100
MIL-118C	1.5	9.6	0.28	47
	5.1	13.2	0.79	53

[a] Accuracy: δ_{iso} (±0.3 ppm); C_Q (±0.2 MHz); η_Q(±0.02); relative area (±8%).

can be hardly distinguished in the 1D spectrum due to its overlap with the external satellite transition of the main signal. This may indicate the presence of a small amount of an aluminum-based impurity. The quantitative estimates of ^{27}Al intensities in MIL-118C phase can be best obtained by combining the analysis of MQMAS and MAS spectra. The MQMAS spectrum (Figure 10), which is not inherently quantitative, can be used to determine the isotropic chemical shift and the quadrupolar parameters for different sites. This provides a starting set of parameters for simulating the MAS spectra in order to obtain the correct intensities. The best fits of the experimental spectra yielding to the simulated spectra showed in Figure 9 were obtained with the parameters presented in Table 2. All signals resonating at around 1−5 ppm are in agreement with octahedrally coordinated aluminum sites. The large C_Q values, on the order of 8−13 MHz, indicate large distortion of the Al environment in MIL-118 frameworks. This could be related to the nature of the rigid directing ligand btec. For comparison, a C_Q of ca. 11 MHz was observed for MIL-69 with 2,6-naphtalenedicarboxylate as ligand,[11] while lower values around 2−8 MHz were found for MIL-110[13] and MIL-96[12] materials employing the higher symmetric trimesate ligand. The C_Q parameter increases progressively after successive transformations of MIL-118 from form A to form C. This reveals the changes occurring in the Al lattice in these materials becoming more and more rigid. The two sites in MIL-118C have distinct quadrupolar parameters, quadrupolar coupling constant C_Q as well as asymmetry parameter η_Q, but equal population in agreement with XRD data. This indicates substantial differentiation between the two Al sites in the structure of MIL-118 induced by strong interactions of water molecules in the channels with the framework.

Figure 11 shows the ^{1}H NMR spectra of the three forms of MIL-118. MIL-118A compound exhibits two strong signals at 2.7 and 7−8 ppm, and two weak resonances at 0.2 and 12.2 ppm. The latter may be due to some impurities present in the sample as extra-framework Al-OH species and residual nonreacting H_4btec, respectively. The signal at 7.5 ppm is actually composite and could be decomposed into two resonances, a broad signal at 7.5 ppm and a narrower signal at 7.3 ppm corresponding to protons of bonded water molecules and protons of aromatic btec moieties, respectively. The signal at 2.7 ppm is therefore assigned to the μ_2-OH bridging group of the network. The intensities ratio of 2:2:3 found for the 2.7, 7.3, and 7.5 ppm signals respectively agree consistently with the expected protons ratio of 2 H/2 H/4 H corresponding to μ_2-OH, btec and H_2O groups in $Al_2(OH)_2(H_2O)_2[C_{10}O_8H_2]$ (MIL-118A). A slight underestimation of the amount of water molecules may come from its broadness. It should be mentioned that this signal of water showed an unusual line-shape. This may be related to the particular interaction of these water molecules with the noncoordinating carboxylate functions through strong hydrogen bondings. Such a proton exchange process may broaden the signal and shift it to higher field. These observations can be further strengthened by the ^{1}H(^{27}Al)

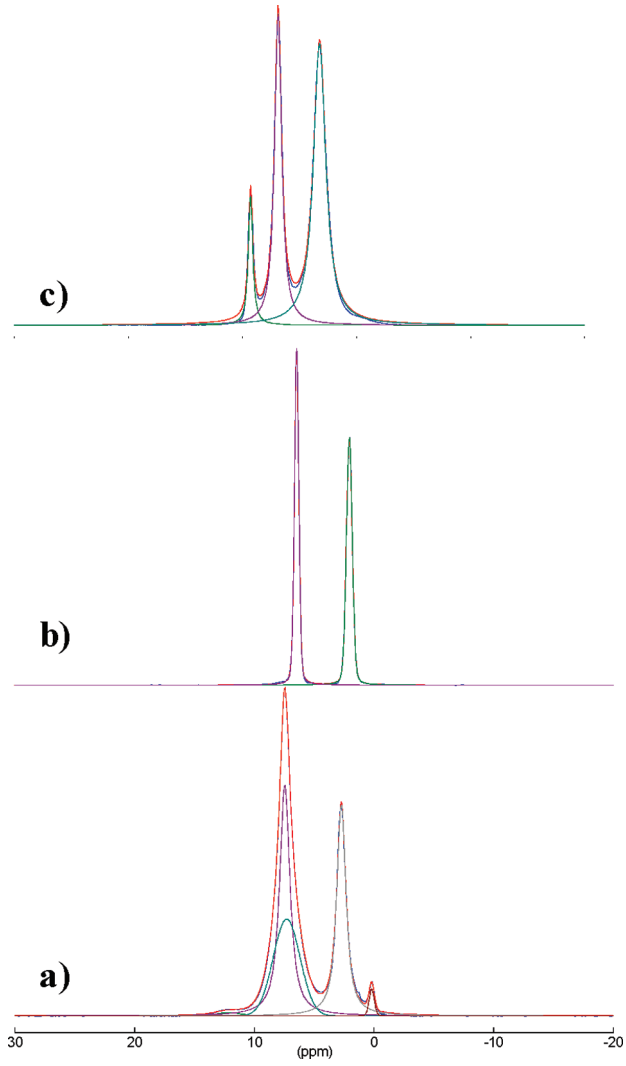

Figure 11. ^{1}H MAS spectra of (a) MIL-118A, (b) MIL-118B, and (c) MIL-118C. All spectra were recorded at 500 MHz and spinning rate 30 kHz.

TRAPDOR spectrum (see Supporting Information). Indeed, ^{1}H(^{27}Al) TRAPDOR experiment is used to probe the proximity between protons of coordinating OH and H_2O and the aluminum sites through ^{1}H−^{27}Al heteronuclear dipolar couplings. The spectrum showed a dominant signal of μ_2-OH as due to strong dipolar Al−H interaction and a weak signal at 7.3 ppm as a result of weaker interaction of water molecules most probably averaged by rotational motion. The spectrum of MIL-118B, upon dehydration, shows two well resolved signals of μ_2-OH at 2.1 ppm and aromatic btec at 6.5 ppm in a 2:2 ratio consistent with the chemical formula of $Al_2(OH)_2[C_{10}O_8H_2]$. The removal of water induces a structural change giving rise to the low-field shifts (0.6−0.8 ppm) of all signals. The spectrum of MIL-118C, after rehydration, changes drastically exhibiting an important structural change. The spectrum shows three distinct signals at 3.2, 6.7, and 9.3 ppm with intensities ratio of 6:4:2, respectively. The assignments are as follows. The signal at 3.2 ppm is due to μ_2-OH and Ow1 water protons, attached to each other, in fast chemical exchange explaining the high-field shift (1.1 ppm) of μ_2-OH relative to MIL-118B. The signal at 6.7 ppm corresponds to the btec aromatic protons. The low-field peak at 9.3 ppm is due to the protons of Ow2 water molecule localized in the center of the channels. On the basis of these assignments, we expect the relative population ratio of 6:2:2

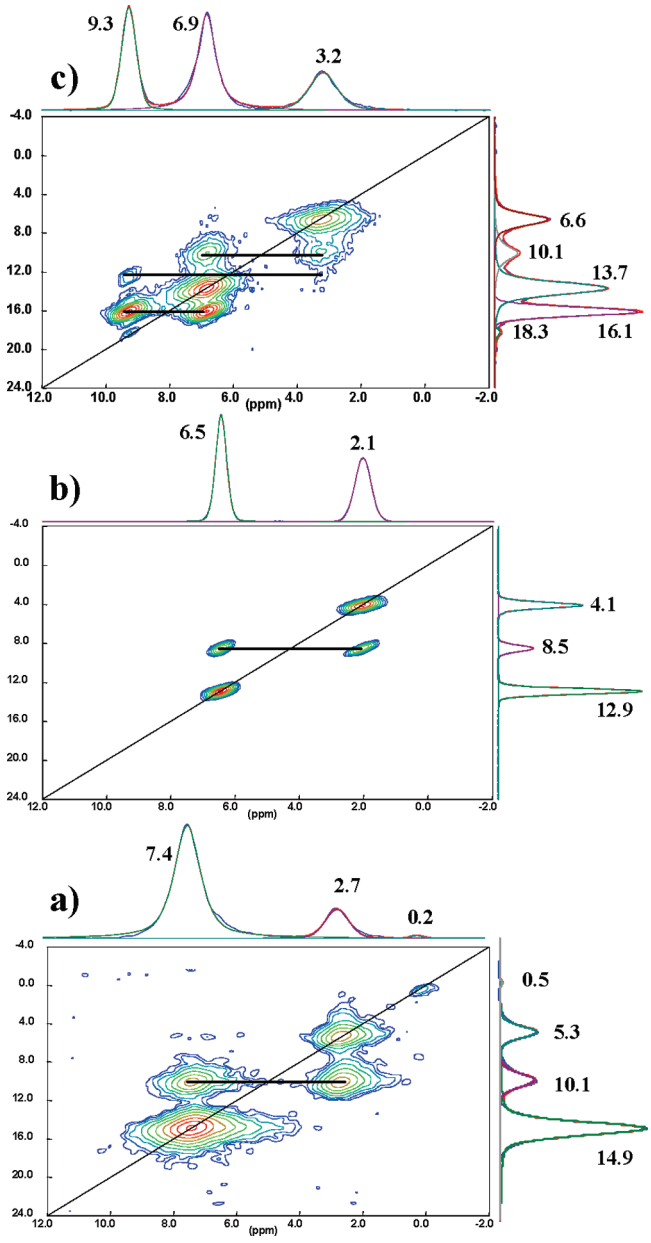

Figure 12. 2D $^1H-^1H$ back-to-back spectrum of (a) MIL-118A, (b) MIL-118B, and (c) MIL-118C. All spectra were recorded with a spinning speed of 30 kHz and four rotor periods for excitation and reconversion.

accounting for 2 H of 2 OH + 4 H of 2 Ow1: 2 H of btec: 2 H of 1 OW2 present in MIL-118C with the chemical formula of $Al_2(OH)_2[C_{10}O_8H_2]\cdot 3H_2O$.

To establish these proton environments in the crystal lattice, in particular, correlations between framework and extra-framework protons, we have carried out a 2D $^1H-^1H$ experiments employing a double quantum (DQ) recoupling sequence back-to-back (BABA[30]). In DQ-SQ 2D spectra, peaks along the F1 = 2F2 correlation line can only arise if there is a dipolar coupling between identical crystallographic sites. Figure 12 shows 2D BABA contour plots of MIL-118 samples. The connectivities between individual proton signals are shown as horizontal lines in Figure 12. The strong correlations between hydroxyl group signals and btec signals for MIL-118A and MIL-118B materials indicate clearly their presence in the same phase. The situation is different for the 0.2 ppm signal in MIL-118A showing only a diagonal signal as an indication of isolated extra-framework species. It is interesting to note, for MIL-118C, the relatively strong cross-peaks between the Ow2 (9.3 ppm) and btec (6.7 ppm) protons, confirming their spatial proximity. The nearest protons of the Ow2 molecules are those carried by the aromatic ring (Ow2-C $\approx$ 3.1 Å). Moreover, the Ow2 points toward oxygen Ow1 with short distances indicating a strong hydrogen bonding. Ow1-Ow2 alternates in making a zigzag chain in the structure linked by hydrogen bonds.

Conclusions

In summary, a 3D MOF-type aluminum pyromellitate (MIL-118) has been hydrothermally synthesized, and its dehydration−rehydration process has been fully characterized by X-ray diffraction (involving single-crystal analysis from microfocused synchrotron beam and ab initio structure determination from powder) and solid-state NMR (^{27}Al and ^1H). MIL-118 framework is built up from infinite trans-connected chains of aluminum-centered octahedra linked to each other through the tetradentate carboxylate ligand. In the as-synthesized compound (MIL-118A), a water molecule attached to aluminum is in a terminal position and involved in strong hydrogen-bond interactions with nonbonded carboxyl oxygen atoms of one carboxylate arm of the pyromellitate linker. Upon heating, the water species is removed and this generates the solid-state formation of an Al-OCO bonding (MIL-118B). At room temperature, the MIL-118 phase is able to sorb ambient water within the channels (MIL-118C), which induces reversibly the shift of inorganic chains to each other, reflecting the flexibility of this rather rigid framework upon guest molecules adsorption. The MIL-118 network illustrates a new example of thermal conversion of hydrogen-bond interactions into covalent bond together with a flexible MOF structures.

Acknowledgment. The authors would like to thank Dr. Eric Leroy and Dr. Michel Latroche (ICMPE, Thiais, France) for their assistance for the SEM images.

Supporting Information Available: The material including cif files, IR spectra, thermodiffractograms, 1H{27Al} TRAPDOR NMR spectrum, and 27Al 3QMAS NMR spectrum is available free of charge via the Internet at http://pubs.acs.org.

References

(1) Férey, G. *Chem. Soc. Rev.* **2008**, *37*, 191.
(2) Kitagawa, S.; Kitaura, R.; Noro, S.-I. *Angew. Chem., Int. Ed.* **2004**, *43*, 2334.
(3) Yaghi, O. M.; O'Keeffe, M.; Ockwig, N. W.; Chae, H. K.; Eddaoudi, M.; Kim, J. *Nature* **2003**, *423*, 705.
(4) Alaerts, L.; Maes, M.; Giebler, L.; Jacobs, P. A.; Martens, J. A.; Denayer, J. F. M.; Kirschhock, C. E. A.; De Vos, D. E. *J. Am. Chem. Soc.* **2008**, *130*, 14170.
(5) Janiak, C. *Dalton Trans.* **2003**, 2781.
(6) Mueller, U.; Schubert, M.; Teich, F.; Puetter, H.; Schierle-Arndt, K.; Pastré, J. *J. Mater. Chem.* **2006**, *16*, 626.
(7) Maspoch, D.; Ruiz-Molina, D.; Veciana, J. *Chem. Soc. Rev.* **2007**, *36*, 770.
(8) Férey, G.; Millange, F.; Morcrette, M.; Serre, C.; Doublet, M.-L.; Grenèche, J.-M.; Tarascon, J.-M. *Angew. Chem., Int. Ed.* **2007**, *46*, 3259.
(9) Chae, H. K.; Siberio-Pérez, D. Y.; Kim, J.; Go, Y. B.; Eddaoudi, M.; Matzger, A. J.; O'Keeffe, M.; Yaghi, O. M. *Nature* **2004**, *427*, 523.
(10) Loiseau, T.; Serre, C.; Huguenard, C.; Fink, G.; Taulelle, F.; Henry, M.; Bataille, T.; Férey, G. *Chem.—Eur. J.* **2004**, *10*, 1373.
(11) Loiseau, T.; Mellot-Draznieks, C.; Muguerra, H.; Férey, G.; Haouas, M.; Taulelle, F. C. R. *Chimie* **2005**, *8*, 765.
(12) Loiseau, T.; Lecroq, L.; Volkringer, C.; Marrot, J.; Férey, G.; Haouas, M.; Taulelle, F.; Bourrely, S.; Llewellyn, P. L.; Latroche, M. *J. Am. Chem. Soc.* **2006**, *128*, 10223.

(13) Volkringer, C.; Popov, D.; Loiseau, T.; Guillou, N.; Férey, G.; Haouas, M.; Taulelle, F.; Mellot-Draznieks, C.; Burghammer, M.; Riekel, C. *Nat. Mater.* **2007**, *6*, 760.
(14) Comotti, A.; Bracco, S.; Sozzani, O.; Horike, S.; Matsuda, R.; Chen, J.; Takata, M.; Kubota, Y.; Kitagawa, S. *J. Am. Chem. Soc.* **2008**, *130*, 13664.
(15) Senkovska, I.; Hoffmann, F.; Fröba, M.; Getzschmann, J.; Kaskel, S. *Microporous Mesoporous Mater.* **2009**, in press.
(16) Barthelet, K.; Riou, D.; Nogues, M.; Ferey, G. *Inorg. Chem.* **2003**, *42*, 1739.
(17) Sanselme, M.; Grenèche, J.-M.; Riou-Cavellec, M.; Férey, G. *Solid State Sci.* **2004**, *6*, 853.
(18) Loiseau, T.; Muguerra, H.; Haouas, M.; Taulelle, F.; Férey, G. *Solid State Sci.* **2005**, *7*, 603.
(19) Volkringer, C.; Loiseau, T.; Férey, G. *Solid State Sci.* **2009**, *11*, 29.
(20) Chu, D.-Q.; Pan, C.-L.; Wang, L.-M.; Xu, J.-Q. *Mendeleev Commun.* **2002**, 207.
(21) Lin, Z.-Z.; Jiang, F.-L.; Chen, L.; Yuan, D.-Q.; Zhou, Y.-F.; Hong, M.-C. *Eur. J. Inorg. Chem.* **2005**, 77.
(22) Lin, Z.-Z.; Jiang, F.-L.; Yuan, D.-Q.; Chen, L.; Zhou, Y.-F.; Hong, M.-C. *Eur. J. Inorg. Chem.* **2005**, 1927.
(23) Tian, Z.; Song, T.; Fan, Y.; Shi, S.; Wang, L. *Inorg. Chim. Acta* **2007**, *360*, 3424.
(24) Sanselme, M.; Riou-Cavellec, M.; Férey, G. *Solid State Sci.* **2002**, *4*, 1419.
(25) Kabsch, W. *XDS in International Tables for Crystallography, Volume F. Crystallography of Biological Macromolecules*; Rossmann, M. G.; Arnold, E., Eds.; International Union of Crystallography: Chester, England, 2001; Chapter 25.2.9.
(26) Sheldrick, G. M. SHELXS-86 -A program for automatic solution of crystal structures. *Acta Crystallogr.* **1990**, *A46*, 467.
(27) Sheldrick, G. M. *SHELX-97 - A Program for Crystal Structure Refinement. Release 97-2*; University of Göttingen: Germany, 1997.
(28) *Topas V4.1: General Profile and Structure Analysis Software for Powder Diffraction Data*; Bruker AXS Ltd.: Conventry, U.K., 2008.
(29) Altomare, A.; Burla, M. C.; Carrozzini, B.; Cascarano, G.; Giacovazzo, C.; Guagliardi, A.; Moliterni, A. G. G.; Polidori, G.; Rizzi, R. *J. Appl. Crystallogr.* **1999**, *32*, 339.
(30) Sommer, W.; Gottwald, J.; Demco, D. E.; Spiess, H. W. *J. Magn. Reson. Ser. A* **1995**, *113*, 131.
(31) Kao, H. M.; Grey, C. P. *J. Phys. Chem.* **1996**, *100*, 5105.
(32) Deng, F.; Yue, Y.; Ye, C. *Solid State Nucl. Magn. Reson.* **1998**, *10*, 151.
(33) Goldbourt, A.; Madhu, P. K.; Vega, S. *Chem. Phys. Lett.* **2000**, *320*, 448.
(34) Brese, N. E.; O'Keeffe, M. *Acta Crystallogr. B* **1991**, *47*, 192.
(35) Loiseau, T.; Muguerra, H.; Marrot, J.; Férey, G.; Haouas, M.; Taulelle, F. *Inorg. Chem.* **2005**, *44*, 2920.
(36) Vittal, J. J. *Coord. Chem. Rev.* **2007**, *251*, 1781.
(37) Ranford, J. D.; Vittal, J. J.; Wu, D. *Angew. Chem., Int. Ed.* **1998**, *37*, 1114.
(38) Ranford, J. D.; Vittal, J. J.; Wu, D.; Yang, X. *Angew. Chem., Int. Ed.* **1999**, *38*, 3498.
(39) Bradshaw, D.; Claridge, J. B.; Cussen, E. J.; Prior, E. J.; Rosseinsky, M. J. *Acc. Chem. Res.* **2005**, *38*, 273.
(40) Ferey, G.; Serre, C. *Chem. Soc. Rev.* **2009**, in press.
(41) Kitagawa, S.; Uemura, K. *Chem. Soc. Rev.* **2005**, *34*, 109.
(42) Liu, Y.; Her, J.-H.; Dailly, A.; Ramirez-Cuesta, A. J.; Neumann, D. A.; Brown, C. M. *J. Am. Chem. Soc.* **2008**, *130*, 11813.
(43) Millange, F.; Serre, C.; Guillou, N.; Férey, G.; Walton, R. I. *Angew. Chem., Int. Ed.* **2008**, *47*, 4100.
(44) Volkringer, C.; Loiseau, T.; Guillou, N.; Férey, G.; Elkaim, E.; Vimont, A. *Dalton Trans.* **2009**, 2241.
(45) Volkringer, C. Ph.D. thesis dissertation; University of Versailles Saint Quentin: France, 2009.

CG900276G